Available online at www.sciencedirect.com
ScienceDirect
Trans. Nonferrous Met. Soc. China 20(2010) 2272−2280
Transactions of Nonferrous Metals Society of China
www.tnmsc.cn

Influence of heat treatment on nanocrystalline zirconia powder and plasma-sprayed thermal barrier coatings

JIANG Xian-liang(蒋显亮)[1], LIU Chun-bo(刘纯波)[1], LIU Min(刘 敏)[2], ZHU Hui-zhao(朱晖朝)[2]

1. School of Materials Science and Engineering, Central South University, Changsha 410083, China;
2. Guangzhou Research Institute of Non-ferrous Metals, Guangzhou 510651, China

Received 23 November 2009; accepted 26 March 2010

Abstract: Nanostructured zirconia top coat was deposited by air plasma spray and NiCoCrAlTaY bond coat was deposited on Ni substrate by low pressure plasma spray. Nanostructured and conventional thermal barrier coatings were heat-treated at temperature varying from 1050 to 1 250 °C for 2−20 h. The results show that obvious grain growth was found in both nanostructured and conventional thermal barrier coatings (TBCs) after high temperature heat treatment. Monoclinic/tetragonal phases were transformed into cubic phase in the agglomerated nano-powder after calcination. The cubic phase content increased with increasing calcination temperature. Calcination of the powder made the yttria distributed on the surface of the nanocrystalline particles dissolve in zirconia when grains grew. Different from the phase constituent of the as-sprayed conventional TBC which consisted of diffusionless-transformed tetragonal, the as-sprayed nanostructured TBC consisted of cubic phase.
Key words: nanocrystalline material; zirconia; thermal barrier coating; heat treatment; phase composition

1 Introduction

Hundreds of different types of coatings are used to protect a variety of structural engineering materials from corrosion, wear, and erosion, and to provide lubrication and thermal insulation. Of all these, thermal barrier coatings (TBCs) have the most complex structure and must operate in the most demanding high-temperature environment of aircraft and industrial gas-turbine engines. TBCs, which comprise metal and ceramic multi-layers, insulate turbine and combustor engine components from the hot gas stream, and improve the durability and energy efficiency of these engines[1].

Plasma-sprayed conventional zirconia TBC, like bulk ceramics, is brittle. The brittleness of the conventional ceramic TBC can be reduced through decreasing grain sizes. Since 1997, a lot of research work on the development of nanostructured zirconia TBC has been conducted worldwide. Coating thickness was varied in the range of 200−1 000 μm. Coating porosity changed from 5% to 20%. Pores were uniformly distributed in the coating under an optimized plasma spray condition[2−3]. The melted agglomerates kept unmelted or partially melted nano-particles together, making the coating be integral[4−5]. Grains grew slowly when heat treatment temperature was below 900 °C and grew fast when temperature was above 900 °C[6]. Average grain size changed from 57 to 88 nm when heat treatment temperature was increased from 600 to 1 150 °C. Average grain size changed from 57 to 177 nm when the nanostructure coating was heat-treated at 1 100 °C for 300 h[7]. Grain growth activation energy in the nanostructured coating is very low and growth mechanism is grain-rotation induced grain coalescence.

The thermal shock behavior of nanostructured zirconia TBC is remarkably different from that of conventional zirconia TBC. For the nanostructured coating, vertical surface cracks were generated after 80 cycles at 1 000 °C, then the cracks slowly propagated toward the top coat/bond coat interface with the increase of cycling number, and finally stopped at the interface[8]. No obvious horizontal crack was found. However, for the conventional coating, obvious horizontal cracking occurred near the top coat/bond coat interface with the increase of cycling number. Nanostructured TBC has better thermal shock resistance and higher thermal

Foundation item: Project(1343-77212) supported by the Innovation Program for Graduate Students of Central South University, China
Corresponding author: JIANG Xian-liang; Tel: +86-731-88876307; E-mail: xljiang@mail.csu.edu.cn
DOI: 10.1016/S1003-6326(10)60640-1

cycling capability than conventional TBC[9−10]. The improvement of the thermal shock resistance is attributed to the formation of a large number of microcracks, uniformly distributed small pores and a large area of nanostructured region with high stress relief capability.

In the agglomerated zirconia powder composed of 8% Y_2O_3 (mass fraction, the same below if not mentioned), major tetragonal phase and minor monoclinic phase were found. After plasma spraying, only tetragonal phase was present in the plasma-sprayed coating. Phase transformation behaviors in nanostructured and conventional TBCs have been investigated. When as-sprayed nanostructured TBC was heat-treated at different temperatures from 600 to 1 150 °C for 15 h and at 1 100 °C for 15−300 h[7, 11], the coatings with and without the heat treatment consisted of tetragonal phase; phase transformation did not occur in the TBC during the heat treatment. As-sprayed conventional TBC was heat-treated at 1 300 °C and 1 500 °C for 100 h and cooled at four different cooling ways, namely water cooling, air cooling, open furnace cooling, and furnace cooling[12]. In the specimens heat-treated at 1 500 °C, yttria stabilized zirconia (YSZ) coating contained some monoclinic phases while none existed in the YSZ coating heat-treated at 1 300 °C. The different phase transformation behaviors at the two temperatures are due to the stabilizer concentration in high temperature phases and grain growth. For YSZ coating specimens heat-treated at 1 500 °C for 100 h, the amount of monoclinic phases increased with slower cooling rates. Tetragonal phases with $c/(a\sqrt{2})$ of 1.017 were considered to be the 'low-stablizer' tetragonal 1 phases (t1), those with $c/(a\sqrt{2})$ of ~1.005−1.007 to be the tetragonal t′ phases, and those with $c/(a\sqrt{2})$ of 1.003 to be the 'high-stablizer' tetragonal 2 phases (t2). After being heat-treated at 1 400 °C for 100 h and then at 1 480 °C for 24 h, a 4.5% (mole fraction) YSZ coating was transformed into two new tetragonal phases: a low-stablizer phase and a high-stablizer zirconia phase with some monoclinic phases formed[13]. Laser glazing was used for the homogenization of local inhomogeneities in Y_2O_3 content and led to the disappearance of the residual monoclinic phase due to rapid cooling[14]. Only the nontransformable t′ phase was present within the melted layers with some variation in preferred orientations. Effect of high temperature calcination on the phase compositions of nanocrystalline zirconia powder and coating was studied. High temperature calcinations made yttria segregated at grain boundaries dissolve in zirconia. Complete cubic phase was obtained in nanostructured TBC[15].

Some challenges for nanostructured TBC to be used in gas turbine engines exist. These challenges include the change of physical and mechanical properties with temperature and time due to the obvious nano-grain growth at high temperatures (>1 200 °C), and the low gas/particle erosion resistance resulting from the low hardness of nanostructured TBC. In this work, the influence of high temperature heat treatment on the microstructures and phase compositions of nanocrystalline zirconia powder and plasma-sprayed nanostructured and conventional zirconia TBCs was investigated.

2 Experimental

Original nanocrystalline zirconia powder was produced by the method of chemical co-precipitation. Its nominal composition was ZrO_2-8% Y_2O_3. Average grain size was about 25 nm. Because of the poor flow ability of the original nano-powder that was unsuitable for plasma spray, the original nano-powder was agglomerated by the method of spray drying. The spray-dried nano-powder was calcined in air from 900 to 1 300 °C for 2 h. Heating rate was approximately 4 °C/min. The calcined nano-powder was cooled in furnace. The powder feedstock used for plasma spray was calcined at 1 250 °C for 2 h and its morphology is shown in Fig.1(a). Spherical, nearly spherical, apple-like, and donut-like agglomerated particles were obtained after the spray drying and calcination. Particle size distribution of the calcined, agglomerated nano-powder is shown in Fig.2. d_{10}, d_{50} and d_{90} can be found in Fig.2. Particle size is in the range of 1−40 μm. Composition of conventional feedstock powder was ZrO_2-7% Y_2O_3. This was a fused and crushed powder (Fig.1(b)). Particle size

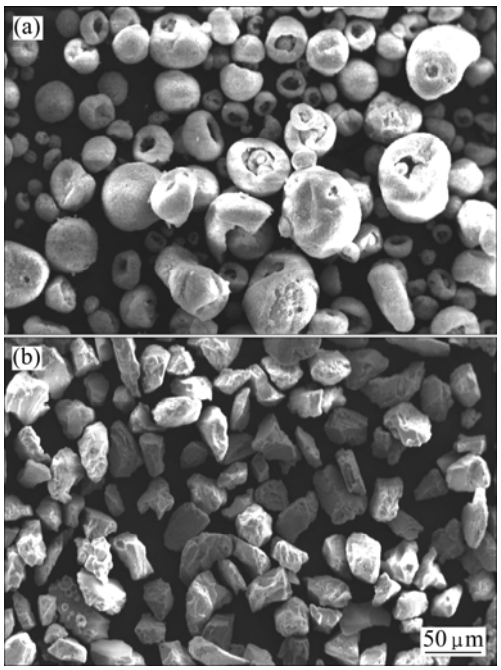

Fig.1 Agglomerated nano-powder feedstock calcined at 1 250 °C for 2 h (a) and conventional powder feedstock (b)

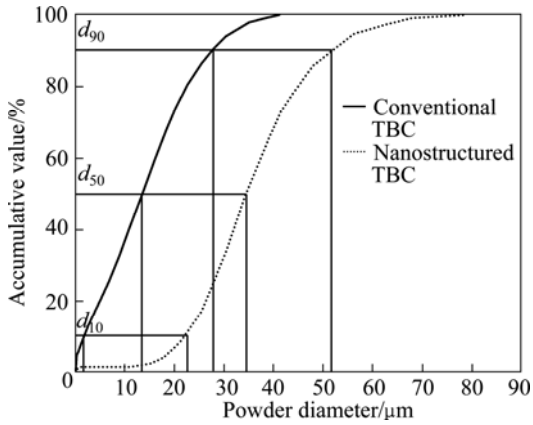

Fig.2 Particle size distribution of agglomerated nano-powder feedstock after calcination and conventional powder feedstock

distribution of the conventional powder is also shown in Fig.2, and the particle size is in the range of 10−80 μm.

Air plasma spray (APS) and low pressure plasma spray (LPPS) were conducted in the Guangzhou Research Institute of Non-ferrous Metals, China. APS facility used was MP-P−1500 model made by GTV Corporation of Germany. LPPS facility used was JZJH-600 model made by the Guangzhou Research Institute. APS parameters for depositing the nanostructured and conventional zirconia coatings are given in Table 1. Thickness of the nanostructured zirconia coating was 150−200 μm. Thickness of the conventional zirconia coating was about 220 μm. Prior to plasma spray forming of the zirconia top coat, a bond coat with the composition of Ni-23.0Co-20.0Cr-9.0Al-4.2Ta-0.6Y (%) was deposited on nickel substrate by LPPS. Thickness of the bond coat was about 100 μm. The metallic bond coat was used in both the nanostructured and conventional TBCs.

Table 1 Air plasma spray parameters for depositing nanostructured and conventional zirconia TBCs

Plasma power/ kW	Spray distance/ mm	Powder feed rate/ ($g\cdot min^{-1}$)	Ar flow rate/ ($L\cdot min^{-1}$)	H_2 flow rate/ ($L\cdot min^{-1}$)
40	100	10−40	40	5

The dimensions of the nanostructured and conventional TBC samples were 60 mm×30 mm×2 mm. Before high temperature heat treatment, the samples were cut into 10 mm×6 mm×2 mm for direct examination under a scanning electron microscope. The high temperature heat treatment was conducted in a box furnace in air. Four pieces of the nanostructured TBC samples were put in one zirconia crucible and three pieces of the conventional TBC samples were put in another crucible. The two crucibles were set in the box furnace before the heat treatment started. Heat treatment temperatures were 1 050, 1 100, 1 150, 1 200, and 1 250 °C. Heat treatment time was 2 h. In addition, the TBC samples were heat-treated at 1 250 °C for 4, 8, and 20 h. During the heat treatment, the furnace was first raised to 1 050 °C at approximately 5 °C/min. After being held at 1 050 °C for 2 h, two crucibles were taken out from the furnace and cooled in air. Then, furnace temperature was raised from 1050 to 1 100 °C in about 30 min (~2 °C/min). After being held at 1 100 °C for another 2 h, another two crucibles were taken out from the furnace and cooled in air. Heat treatment continued in this way until heat treatment at 1 250 °C was completed.

The TBC samples were characterized by a scanning electron microscope (SEM, KYKY−2800, Beijing Instrument Inc., China) and a field emission scanning electron microscope (FESEM, Sirion−200, Phillips, Netherlands). Powder samples were observed by a transmission electron microscope (TEM, Tecnai G^2 20 ST, Phillips, the Netherlands). Phase analysis was performed on a X-ray diffraction instrument (XRD, D/Max−2550, Rigaku, Japan). Cu K_α radiation was used. X-ray diffraction conditions were 1.540 51 Å of wavelength, 40 kV of accelerating voltage, 250 mA of current, 0.02° of step length, and 8 (°)/min of scanning speed.

3 Results and discussion

3.1 Microstructures of as-sprayed nanostructured TBC

The surface morphology of the as-sprayed nanostructured TBC is shown in Fig.3. Three types of heating/melting states of the nano-particles agglomerates were found from the coating surface: fully melted state, partially melted state, and unmelted state. For example, the state of partially melted agglomerates, indicated in Fig.3(b), was determined on the basis of the original nano-particles feature preserved in the coating. Unmelted agglomerates and new nanocrystalline grains formed from fully melted agglomerates are illustrated in Fig.3(c). Unmelted agglomerates kept the feature of nano-powder. Fully melted agglomerates lost the feature of nano-powder. The three types of heating/melting states of the nano-particles agglomerates injected into plasma can be explained by the characteristics of plasma. It is known that plasma has different viscosities, velocities and temperatures along radial and axial directions. In plasma spray, powders are injected into plasma by a carrier gas. The particles with different particle sizes will have different momentums and thus, have different trajectories in plasma and experience different heating rates. Some particles that can pass through the highest temperature zone in plasma will be heated effectively and thus, they will be melted; other particles that cannot pass through the highest temperature zone

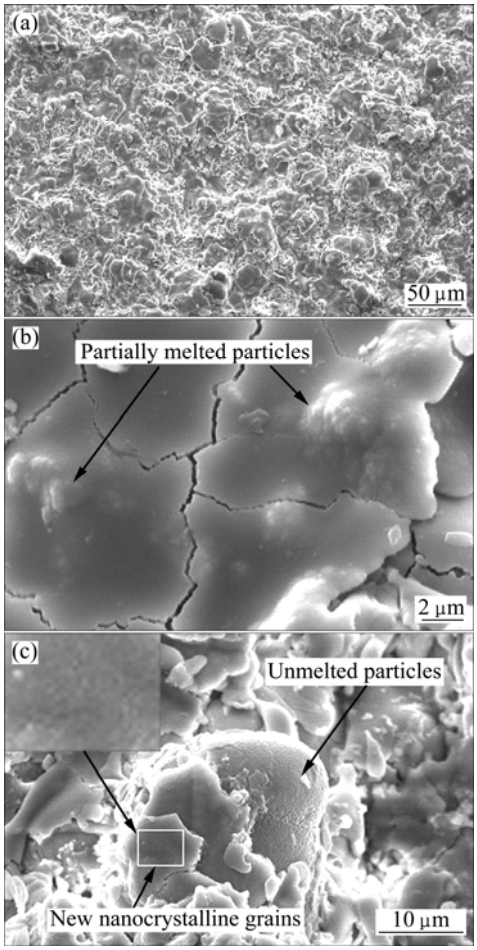

Fig.3 SEM micrographs of as-sprayed nanostructured TBC showing surface morphology (a), partially melted particles (b) and new nanocrystalline grains (c)

in plasma will not be heated effectively and thus, they will not be melted.

3.2 Microstructures of nanostructured and conventional TBCs after high temperature heat treatment

The surface morphologies of the nanostructured TBC heat-treated at 1 250 °C for 2 and 20 h are shown in Fig.4. Compared with the surface morphology of as-sprayed nanostructured TBC, no obvious change in surface morphology can be found from low magnification micrographs. At high magnifications, however, the healing of microcracks can be found. These microcracks became small, resulted from the sintering of the zirconia top coat at high temperatures. Grain growth is clearly illustrated in Fig.4(d). New nanocrystalline grains have grown to about 800 nm after 20 h heat treatment at 1 250 °C. The surface morphology of the conventional TBC heat-treated at 1 250 °C for 20 h is shown in Fig.5. Grain growth in the conventional zirconia TBC is also evident. The grains in some areas have grown into being polyfaceted and grain size has reached 1−2 μm.

SEM micrographs of the cross sections of the nanostructured and conventional TBCs heat-treated at 1 250 °C for 2 h and 20 h are shown in Fig.6. Thermally grown oxide (TGO) formed along the rough interface between the top coat and bond coat. No spallation along the interface was observed and no vertical/horizontal large crack was found in both the nanostructured and conventional TBCs even after being heat-treated at 1 250 °C for 20 h. Although sintering of zirconia top coat occurred, no obvious change in porosity was found. Breaking up of the nanostructured TBC splats into small particles was observed during the grinding and polishing of the TBC samples, as shown in Fig.6(b). However, breaking up of the conventional TBC splats into small particles was not observed. This phenomenon tells us that the cohesive strength of the nanostructured TBC is lower than that of the conventional TBC. It is anticipated that the low cohesive strength of the nanostructured TBC could become an obstacle for future application of the nanostructured TBC to gas turbine engines where strong brush by high velocity stream is present.

3.3 Phase constituents of nanostructured and conventional TBCs before and after high temperature heat treatment

X-ray diffraction patterns of the original nanocrystalline ZrO_2-8% Y_2O_3 powder, the agglomerated nano-powders calcined at 1 100 °C and 1 250 °C, and the as-sprayed nanostructured TBC are shown in Fig.7. According to PDF#30—1468, cubic (400) peak should be at 73.660°. According to PDF#48—0224, tetragonal (004) peak and (220) peak should be corresponding to 73.202° and 74.230°, respectively. Careful examination of the angle (2θ) zoomed from 72° to 76° (Fig.7(c)) did not find the existence of cubic (400) peak in the original nanocrystalline powder, indicating that the original nanocrystalline zirconia powder consisted of monoclinic phase (m) and tetragonal phase (t). As shown in Fig.7(b) and Fig.7(c), the relative heights of the monoclinic, tetragonal and cubic peaks from the original nano-powder and the powders calcined at 1 100 °C and 1 250 °C have changed, indicating that phase transformation occurred during high temperature calcination.

Transmission electron microscopy analysis reveals that a part of yttria was distributed on the surface of original nanocrystalline zirconia particles, as shown in Fig.8(a). After high temperature calcination at 1 250 °C the nano-ziconia particles coalescenced and grew from approximately 25 nm to 200 nm while yttria was dissolved in zirconia. As shown in Fig.8(b), yttria on the surface of zirconia particles almost disappeared. The

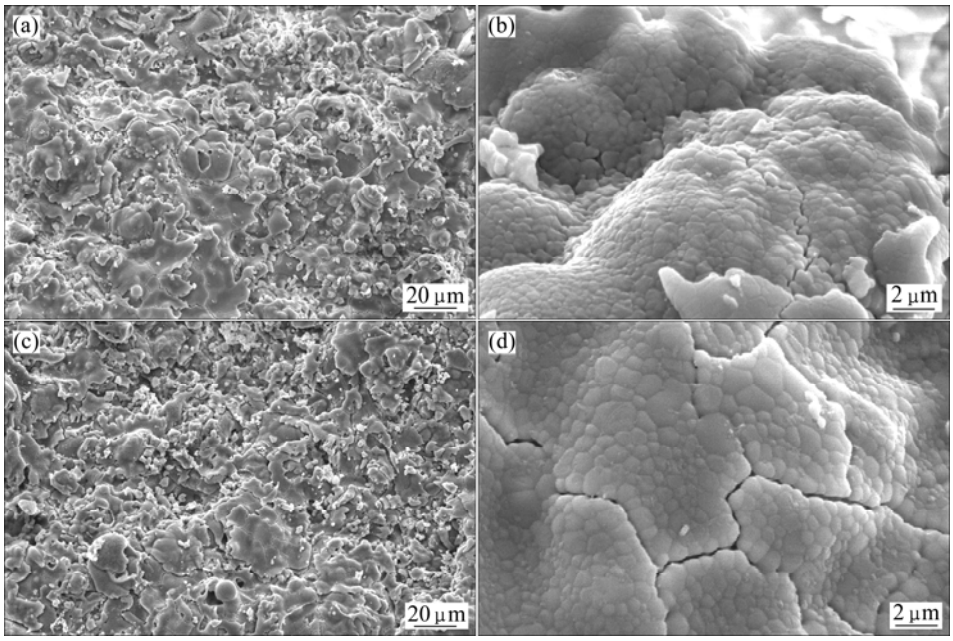

Fig.4 Surface morphologies of nanostructured TBC heat-treated at 1 250 °C for 2 h (a) and (b), and 20 h (c) and (d)

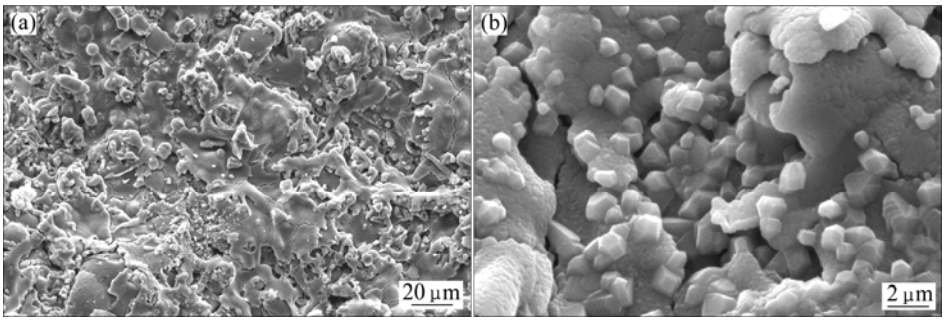

Fig.5 Surface morphologies of conventional TBC heat-treated at 1 250 °C for 20 h

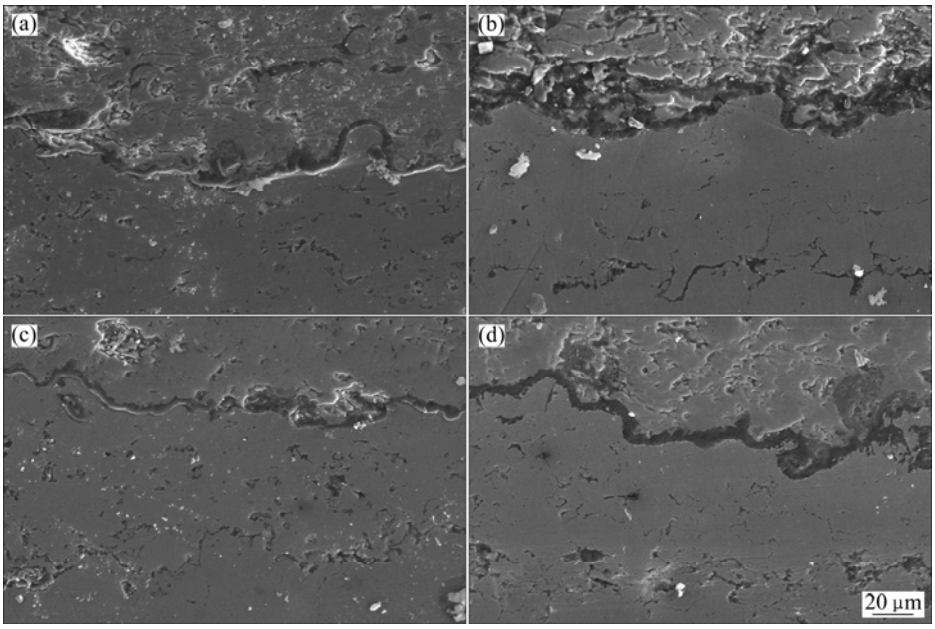

Fig.6 Cross-sectional microstructures of TBCs heat-treated at 1 250 °C for different time: (a) Nanostructured TBC heat-treated for 2 h; (b) Nanostructured TBC heat-treated for 20 h; (c) Conventional TBC heat-treated for 2 h; (d) Conventional TBC heat-treated for 20 h

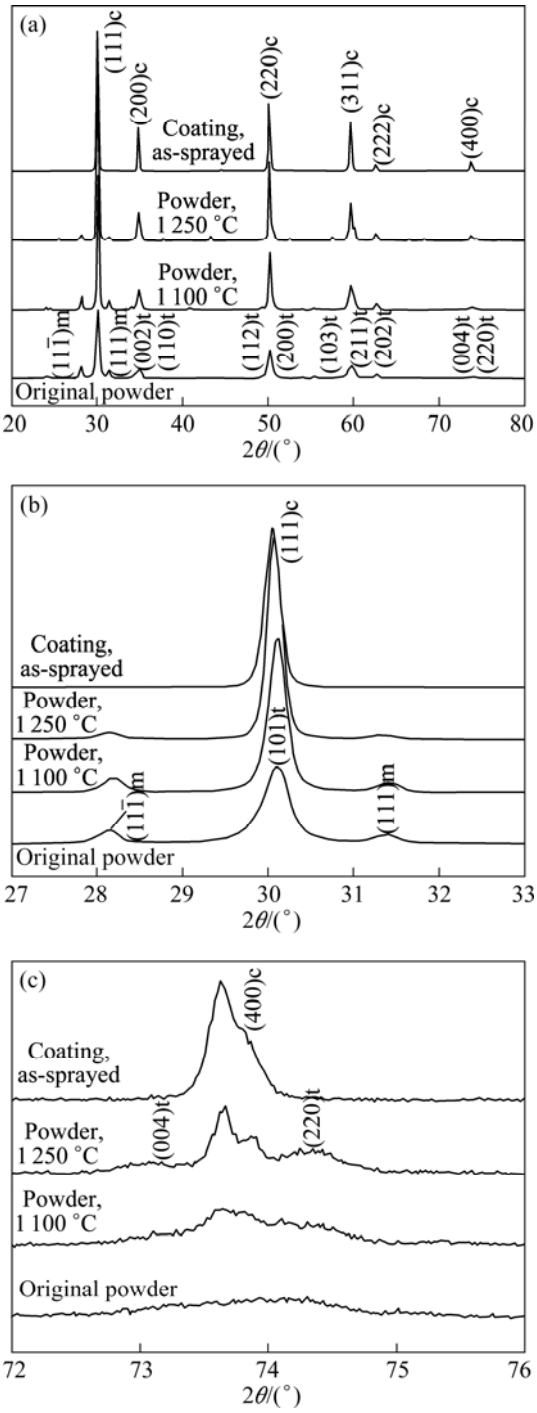

Fig.7 XRD patterns of nano-powder feedstocks before and after calcination at 1 100 °C and 1 250 °C for 2 h, and as-sprayed nanostructured TBC: (a) Whole pattern; (b) 2θ from 27° to 33°; (c) 2θ from 72° to 76°

dissolution of yttria in zirconia lead to the transformation from monoclinic phase to tetragonal phase and further to cubic phase.

The contents of monoclinic, tetragonal and cubic phases in the original and calcined nanocrystalline powders were calculated. The calculation results are given in Table 2. Original nanocrystalline zirconia

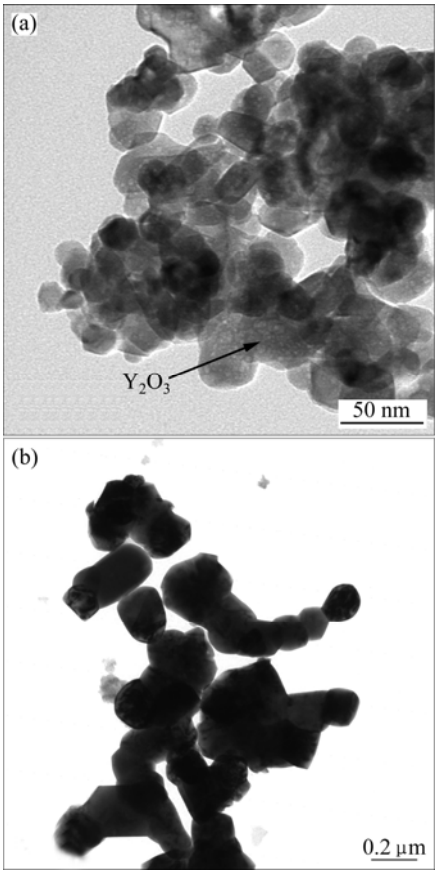

Fig.8 TEM micrographs of nanocrystalline zirconia powders: (a) Original powders; (b) Calcined at 1 250 °C for 2 h

powder was composed of 22.97% monoclinic phase and 77.03% tetragonal phase. After high temperature calcination, cubic phase formed. The contents of the monoclinic phase and tetragonal phase decreased and the content of cubic phase increased as the calcination temperature increased. At 1 250 °C, the powder was composed of 9.84% monoclinic phase, 25.16% tetragonal phase and 65.00% cubic phase. This result tells us that the major phase in the nano-powder feedstock calcined at 1 250 °C for 2 h is cubic rather than tetragonal.

Table 2 Phase contents in original and calcined nanocrystalline zirconia powders

Calcination temperature/°C	Mass fraction of monoclinic phase/%	Mass fraction of tetragonal phase /%	Mass fraction of cubic phase/%
Original	22.97	77.03	0.00
900	19.41	66.88	13.71
1 000	14.98	47.23	37.79
1 100	13.36	31.90	54.74
1 200	9.94	16.18	73.88
1 250	9.84	25.16	65.00
1 300	6.72	11.18	82.10

Phase transformation occurred during plasma spray forming of nanostructured TBC. All of the XRD peaks from the as-sprayed nanostructured TBC shown in Fig.7 are in accordance with PDF#30—1468. This is a cubic phase. Composition of the cubic phase is Y0.15Zr0.85O1.93. This result tells us that all monoclinic/tetragonal phases in the nano-powder feedstock have transformed to cubic phase in the coating during plasma spraying and the cubic phase has been preserved at room temperature.

X-ray diffraction patterns of the conventional zirconia powder and as-sprayed TBC are shown in Fig.9. In Fig.9(c), the two peaks of tetragonal (220) came from the reflection of Cu $K_{\alpha 1}$ and Cu $K_{\alpha 2}$[16]. The conventional zirconia powder consisted of monoclinic and tetragonal phases. The phase constituent is similar to that of the original nanocrystalline zirconia powder, but is different from that of the calcined, agglomerated nano-powder. During plasma spraying of the conventional TBC, phase transformation also occurred. All of the peaks of the as-sprayed conventional TBC are in accordance with PDF#48—0224. Composition of this phase is Y0.08Zr0.92O1.96. This is a tetragonal phase, but is diffusionless-transformed tetragonal phase (t′) due to the rapid cooling of heated/melted particles, on the basis of $c/(a\sqrt{2})$ value (Table 3) which was calculated according to formula (1):

$$\frac{\lambda}{2\sin\theta}=\frac{a}{\sqrt{h^2+k^2+\dfrac{l^2}{(\dfrac{c}{a})^2}}} \tag{1}$$

where λ is the diffraction wavelength; θ is the diffraction angle; α and c are lattice constants of tetragonal phase; h, k, l are index of reflection planes.

Table 3 Lattice constants of tetragonal phase in as-sprayed and heat-treated conventional zirconia TBC, calculated on the basis of (004)t and (220)t reflections

Heat treatment temperature/°C	a, b/nm	c/nm	$c/(a\sqrt{2})$
As-sprayed	0.361 44	0.516 40	1.010 26
1 050	0.361 44	0.517 12	1.011 67
1 100	0.361 42	0.516 92	1.011 34
1 150	0.361 50	0.517 28	1.011 82
1 200	0.361 53	0.517 24	1.011 66
1 250	0.361 61	0.517 28	1.011 51

XRD patterns of the nanostructured TBC heat-treated from 1 050 to 1 250 °C for 2 h are shown in Fig.10. All of these peaks in the XRD pattern are corresponding to those of cubic phase. No obvious phase transformation occurred when the as-sprayed nanostructured TBC samples were heat-treated at a temperature range of 1 050−1 250 °C. Also, no obvious phase transformation occurred at 1 250 °C when heat treatment time varied from 2 to 20 h, as shown in Fig.11. The phase composition of the as-sprayed nanostructured TBC was not changed. The cubic phase is stable at high temperatures.

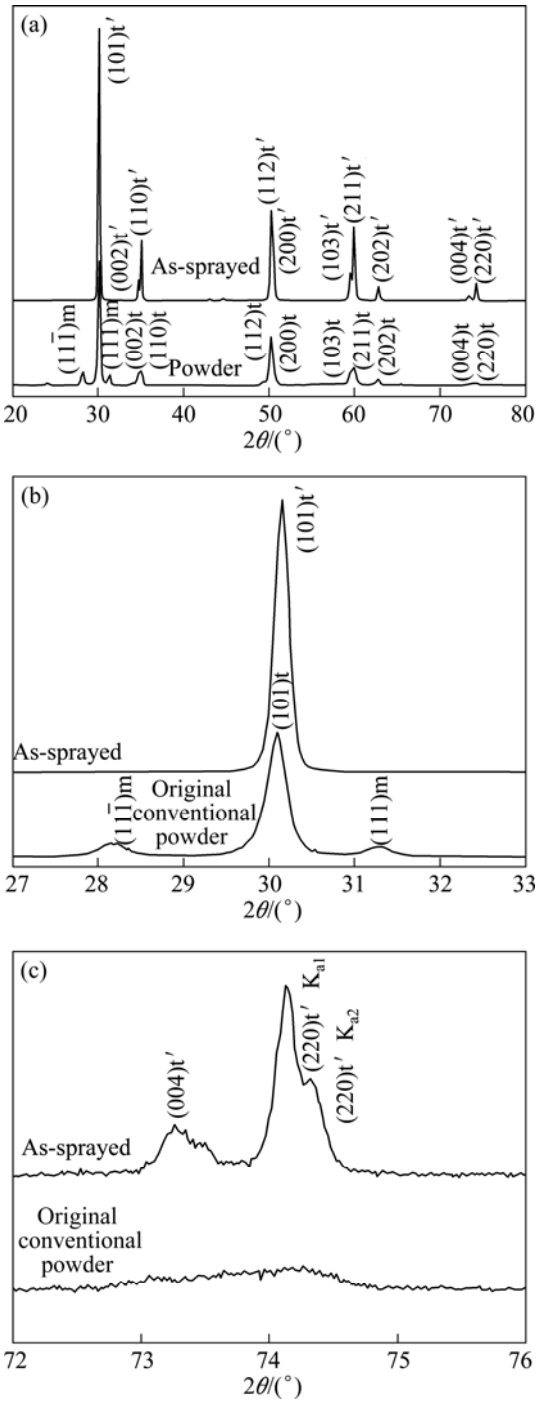

Fig.9 XRD patterns of conventional powder feedstock and as-sprayed conventional TBC: (a) Whole pattern; (b) 2θ from 27° to 33°; (c) 2θ from 72° to 76°

XRD patterns from the conventional TBC heat-treated from 1 050 to 1 250 °C for 2 h are shown in Fig.12. There is no cubic phase presented in the heat-treated conventional TBC. There is almost no change of $c/(a\sqrt{2})$ with the variation of heat treatment temperature, as given in Table 3. The diffusionless-transformed tetragonal phase (t′) did not decompose into equilibrium tetragonal (t) and cubic (c) phases. No phase transformation occurred when heat treatment time at 1250 °C increased from 2 to 20 h, as shown in Fig.13.

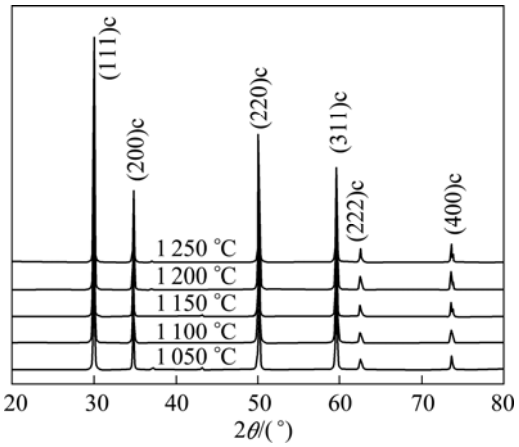

Fig.10 XRD patterns of nanostructured TBC heat-treated for 2 h at different temperatures

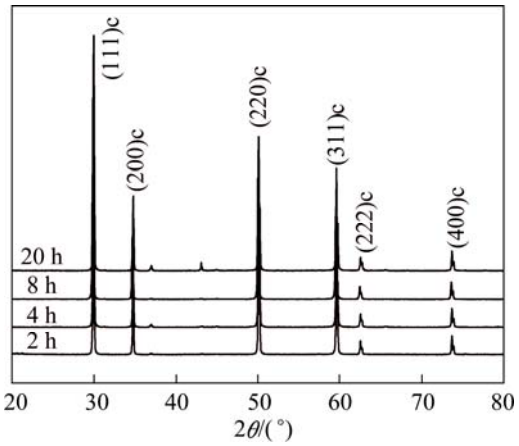

Fig.11 XRD patterns of nanostructured TBC heat-treated at 1 250 °C for different time

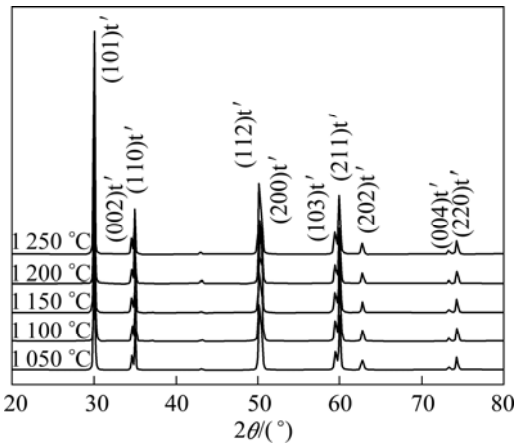

Fig.12 XRD patterns of conventional TBC heat-treated for 2 h at different temperatures

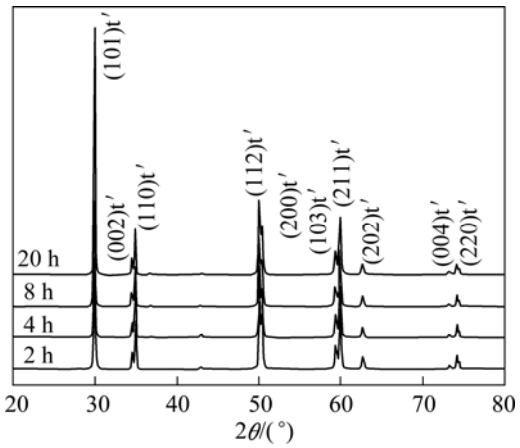

Fig.13 XRD patterns of conventional TBC heat-treated at 1 250 °C for different time

4 Conclusions

1) Air plasma spray of agglomerated nanocrystalline zirconia powder results in a large fraction of partially melted particles and a small fraction of fully melted particles under the plasma spray condition. Obvious grain growth is found in both nanostructured and conventional TBCs after high temperature heat treatment.

2) Monoclinic/tetragonal phases in the nanocrystalline zirconia powder are transformed into cubic phase when the powder is calcined at high temperatures. More cubic phase forms as calcination temperature increases.

3) Different from the phase constituent of the as-sprayed conventional TBC which consists of diffusionless-transformed tetragonal, the as-sprayed nanostructured TBC consists of cubic phase when the calcined nanocrystalline zirconia powder is used as feedstock. The influence of heat treatment temperature from 1 050 to 1 250 °C and heat treatment time from 2 h to 20 h on the phase compositions of both nanostructured and conventional TBCs is not evident.

References

[1] PADTURE N P, GELL M, JORDAN E H. Thermal barrier coatings for gas-turbine engine applications [J]. Science, 2002, 296(5566): 280−284.

[2] CHEN Huang, ZHOU Xia-ming, DING Chuan-xian. Investigation of the thermomechanical properties of a plasma-sprayed nanostructured zirconia coating [J]. Journal of the European Ceramic Society, 2003, 23(9): 1449−1455.

[3] LIN Feng, YU Yue-guang, JIANG Xian-liang, ZENG Ke-li, REN

Xian-jing, LI Zhen-duo. Microstructures and properties of nanostructured TBCs fabricated by plasma spraying [J]. The Chinese Journal of Nonferrous Metals, 2006, 16(3): 482−487. (in Chinese).

[4] LIMA R S, KUCUK A, BERNDT C C. Integrity of nanostructured partially stabilized zirconia after plasma spray processing [J]. Materials Science and Engineering A, 2001, 313(1/2): 75−82.

[5] LIMA R S, KUCUK A, BERNDT C C. Evaluation of microhardness and elastic modulus of thermally sprayed nanostructured zirconia coatings [J]. Surface and Coatings Technology, 2001, 135(2/3): 166−172.

[6] WANG Zhen-bo, ZHOU Chun-gen, XU Hui-bin, GONG Sheng-kai. Effect of thermal treatment on the grain growth of nanostructured YSZ thermal barrier coating prepared by air plasma spraying [J]. Chinese Journal of Aeronautics, 2004, 17(2): 119−123.

[7] WANG Na, ZHOU Chun-gen, GONG Sheng-kai, XU Hui-bin. Heat treatment of nanostructured thermal barrier coating [J]. Ceramics International, 2007, 33(6): 1075−1081.

[8] LIANG Bo, DING Chuan-xian. Thermal shock resistances of nanostructured and conventional zirconia coatings deposited by atmospheric plasma spraying [J]. Surface and Coatings Technology, 2005, 197(2/3): 185−192.

[9] ZHOU Chun-gen, WANG Na, WANG Zhen-bo, GONG Sheng-kai, XU Hui-bin. Thermal cycling life and thermal diffusivity of a plasma-sprayed nanostructured thermal barrier coating [J]. Scripta Materialia, 2004, 51(10): 945−948.

[10] LIU Chun-bo, ZHANG Zhi-min, JIANG Xian-liang, LIU Min, ZHU Zhao-hui. Comparison of thermal shock behaviors between plasma-sprayed nanostructured and conventional zirconia thermal barrier coatings [J]. Transactions of Nonferrous Metals Society of China, 2009, 19(1): 99−107.

[11] WANG Na, ZHOU Chun-gen, GONG Sheng-kai, XU Hui-bin. Influence of annealing on the grain growth and thermal diffusivity of nanostructured YSZ thermal barrier coating [J]. Journal of Materials Science and Technology, 2006, 22(6): 793−797.

[12] MOON J, CHOI H, KIM H, LEE C. The effects of heat treatment on the phase transformation behavior of plasma-sprayed stabilized ZrO_2 coatings [J]. Surface and Coatings Technology, 2002, 155(1): 1−10.

[13] LEONI M, JONES R L, SCARDI P. Phase stability of scandia–yttria-stabilized zirconia TBCs [J]. Surface and Coatings Technology, 1998, 108−109(1/3): 107−113.

[14] BATISTA C, PORTINHA A, RIBEIRO R M, TEIXEIRA V, COSTA M F, OLIVEIRA C R. Morphological and microstructural characterization of laser-glazed plasma-sprayed thermal barrier coatings [J]. Surface and Coatings Technology, 2006, 200(9): 2929−2937.

[15] JIANG Xian-liang, LIU Chun-bo, YU Lian-sheng, LIU Min, ZHU Zhao-hui. Effect of high temperature calcination on the phase compositions of nanocrystalline zirconia powder and coating[C]// Proceedings of International Thermal Spray Conference. Las Vegas, 2009: 28−33.

[16] LIANG Bo, DING Chuan-xian, LIAO Han-lin, CODDET C. Phase composition and stability of nanostructured 4.7 wt.% yttria-stabilized zirconia coatings deposited by atmospheric plasma spraying [J]. Surface and Coatings Technology, 2006, 200(14/15): 4549−4556.

(Edited by LI Xiang-qun)